JJMIE

Volume 2, Number 1, Mar. 2008
ISSN 1995-6665
Pages 15 - 21

Jordan Journal of Mechanical and Industrial Engineering

Temperature Dependence of Dynamic Modulus and Damping in Continuous Fiber- Reinforced Al-(alloy) Matrix Composites at Elevated Temperatures

Ramadan J. Mustafa *

Faculty of Engineering, Mu'tah University, Karak, Jordan

Abstract

Mechanical damping (in the longitudinal vibration mode only) and temperature dependence of dynamic modulus in the longitudinal (*II*) and transverse ($\perp$) fiber direction were measured for several metal matrix composites. The piezoelectric ultrasonic oscillator technique was used to generate ultrasonic stress waves for longitudinal measurements at 80 and 150 kHz. Tests were conducted at room temperature and at elevated temperatures up to 450°C and strain amplitudes in the range of 10^{-7} to10^{-2}. The Metal Matrix Composites (MMC's) studied include Al_{pure} and Al(6061) alloy metal matrix reinforced continuous alumina (Al_2O_3), tungsten (w), high strength carbon (H.S.C), boron(B), and silicon carbide (SiC) fibers. The w-Al composite material showed a strain amplitude dependent damping at room temperature, while the Al2O3, B and SiC fiber reinforced Al_{alloy} matrix composites exhibited essentially amplitude independent over a strain range of 10^{-7} to 10^{-4} and a slight nonlinear amplitude dependent damping at higher strain amplitudes. Increasing the area of fiber-matrix interface in H.S.C-Al matrix composites appeared to increase damping in such composites. The measured longitudinal vibration mode damping for H.S.C-Al_{pure} matrix composite at temperature in the range of 25 to 350 ºC has shown to exhibit strain amplitude dependent damping. The temperature dependence of dynamic modulus in the tested composites showed a linear, monotonic decrease in modulus with increasing temperature, except in the case of H.S.C fiber reinforced Al matrix composites which showed a non-monotonic decrease in modulus as temperature increased from room temperature to 450°C. It is suggested that this behavior is caused by residual stresses at the fiber-matrix interface. The flaws detected by ultrasonic flaw detection techniques in the tested composite plates did not significantly affect the modulus as the fibers carry the majority of load in the longitudinal fiber direction. Additionally, the weak fiber-matrix interfacial strength, matrix ductility, and the flaws, which are a potential source of sliding friction and energy absorbing mechanisms, did affect the damping in tested MMC's specimens under longitudinal fiber vibration.

Keywords: Continuous Fibre-Reinforced Al-(alloy) Composites, elevated temperatures, dynamic modulus, dynamic damping;

Nomenclature

d	crystal drive
g	crystal gauge
λ	wavelength of longitudinal wave in component
p	specimen piece
RL	resonant length
EC	Modulus of composite material
ρ_c	density of composite material
f	frequency
c.s.r	ceramic spacer rod
Vg	gauge crystal voltage
ε_{amp}	maximum strain amplitude
V_d	drive gauge crystal voltage
R_{pd}	Resonant period of component
L	length of specimen
E_d	dynamic Young's Modulus of component
$R_{c.s.r}$	Resonant period of component (ceramic spacer rod)
T	temperature of specimen component
C.T.E	coefficient of thermal expansivity
m (i)	mass of component i
σ_f	fracture strength of component
$\sigma_{tensile}$	tensile strength of component

1. Introduction

The knowledge of internal friction and dynamic modulus of materials is important in the field of science and engineering. This knowledge of temperature

* Corresponding author. e-mail: dnimir@yahoo.co.uk

dependence of dynamic modulus can be critical in studies of buckling, stress-strain relations, and fracture mechanics, while in materials science studies, the modulus is related to inter-atomic forces, creep, thermal stresses, etc. Although damping measurements have technological applications in noise and vibration reduction and are extremely useful in fundamental investigations of defects in materials, as material scientists, engineers and designers, seek to understand the structure-property relationships for advanced engineering materials better, the temperature dependence of dynamic modulus and damping at elevated temperature studies is of prime importance.

Furthermore, metal matrix composites are used nowadays in aerospace, automobile industries, and load-bearing structural components, such as fuselage structures in newly developed aircrafts, because of their high specific strength, specific modulus , higher temperature capabilities and better wear resistance, [1,2], than most polymer matrix composites. Aluminum and its alloys are used as matrix materials because of their relatively low densities and good corrosion resistance, [3]. Continuous fiber reinforcement silicon carbide (SiC), high strength carbon fibre (H.S.C), boron (B), alumina (Al_2O_3), and tungsten (w), are of low cost, high performance reinforcements for Aluminum matrix composites since it possesses high temperature stability and it is compatible with molten aluminum.

This paper discusses the results from an ongoing study of the dynamic longitudinal Young's modulus of several metal matrix composites as a function of temperature for relatively small specimens, using the piezoelectric ultrasonic technique, [8-12]. This is ideal for obtaining longitudinal modulus values since it is a dynamic technique, employing ultrasonic stress waves generated by piezoelectric transducers attached to small specimens, during which the specimen temperature is varied from room temperature to 450°C. This versatile technique for making simultaneous measurements of damping, strain amplitude as function of temperature will also be employed for the tested MMC's. The study will examine the strain amplitude dependence of damping, the temperature dependence of dynamic modulus at temperatures in the range of 25 to 450 °C. Through these studies, some insight into the effects of the structure of tested MMC's on damping and modulus properties should be gained that will be useful in future research and design of these high performance materials.

Fracture behavior characterization and prediction have been extensively studied with reference to metals. In the case of composite materials, in general, the fracture behavior (at room temperature) experimental data of destructive testing and prediction models have to some degree been available in the literature, [4-8]. However, a renewed interest in nondestructive testing techniques (such as ultrasonic testing) has been shown to be aimed at providing direct information useful for the assessment of mechanical behavior such as damping and dynamic modulus (at room and at elevated temperatures). Studies on the comparison of different experimental techniques for determination of elastic properties of fiber reinforced and unreinforced metal matrix materials, [9,10], have shown that there is a good agreement between modulus values obtained using four point bending test and ultrasonic technique. This capability of the ultrasonic technique can be used as a method of testing allowing for real time decision making on the development of the applications of composite materials, [8-15], in noise and vibration reduction, and dynamic properties in the material under control.

2. Experimental

2.1. Materials

The metal matrix composites utilized in this study were made of cylindrical specimens of 99.995% pure aluminum (Al_{pure}) and aluminum alloy (6061) (Al_{alloy}) matrix material reinforced with continuous alumina (Al_2O_3), tungsten (w), boron (B), silicon carbide (SiC), and high strength carbon (H.S.C) fibers were used. The MMC's were fabricated using a hot consolidation technique of laid up well-coated fiber-matrix tapes of Al_{pure} and Al_{alloy}) matrix coated with Al_2O_3, w, B, SiC, and H.S.C continuous fibers.

The coatings of fiber-matrix tapes were in the range of 100 μm thickness and were deposited on fibers to produce, on consolidation, MMC's with volume fraction of 25-70%. The cutting up of suitable lengths of the fiber tape were stacked unidirectional in a cylindrical graphite die and hot consolidation process were carried out at 520 º C, pressure of 6 MPa for Al_{pure} matrix coated fibers, and 540 º C at 6 MPa pressure for Al(6061) matrix coated fibers. A consolidation time of 60 minutes were required to produce specimens of 20-40 mm long. Details of the fabrication process can be found in [5].

The mechanical properties of the selected continuous fiber reinforcement and metal matrix materials are shown in Tables 1 and 2, [16-18]

Table 1: The mechanical properties of continuous fiber reinforcement manufacturer specifications and ref [16, 17].

Fiber type	C.T.E (α_f) ($K^{-1}x10^6$)	E (GPa)	σ_f (GPa)	Diameter (μm)	Specific gravity
HSC (Y/C)	-0.4-1.2	270	4.2	7-30	1.9
α-Al_2O_3	7	380	1.5	15-25	3.9
SiC (Y/C)	4.5	190-200	2.5	12	2.6
Boron(B)	8	400	3.5	150	2.6
Tungsten(W)	5	400	2.5	10-150	19.2

Table 2: The mechanical properties of matrix material ref [18]

Material	E (GPa)	$\sigma_{tensile}$ (MPa)	σ_{yield} (MPa)	Strain to failure	Poisson ratio (ν)
99.995 % Al_{pure}	69	90	34	50-70	0.33
Al_{alloy} (6061)	72	310	275	12	0.33

2.2. Testing Procedure

The required lengths of the specimen were estimated using an initial estimate of modulus. Figure 1 shows the basic features of experimental arrangement, namely two piezoelectric quarts crystals as the drive (d) and gauge (g). These crystals are cemented together using a loctite adhesive. Under suitable electrical excitation, the crystals

produce longitudinal, resonant ultrasonic stress waves (wavelength, λ) in the specimen piece (p) of resonant length attached to the gauge crystal. The resonant lengths R_L were estimated using the standard equation ref [18];

$$R_L = \frac{1}{2f}\sqrt{\frac{E_c}{\rho_c}} = \frac{\lambda}{2} \qquad (1)$$

Where E_c is the longitudinal modulus of composite specimen and ρ_c is the estimated density of the composite specimen type used for the tests, and *f* is the frequency, controlled by the length of the quarts crystals of up to 200 kHz. A typical length of specimens of 20-40 mm was chosen for all tests.

For room temperature tests, as in Fig.1, the specimen was adhered to the end of the gauge crystal using a loctite type of adhesive material.

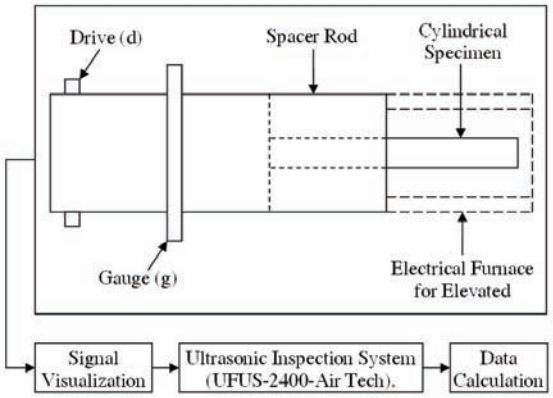

Fig. 1: Schematic diagram showing the four component system used for measurements at elevated temperatures (or at room temperature by removing the electrical furnace).

For elevated temperature testing, a ceramic (such as quartz) spacer rod (c.s.r) had to be cut and glued between the crystals and the specimen, and at high temperature testing the piezoelectric probes were also shielded and cooled by air.

After the specimen (p) had stabilized at the desired temperature (30-35 minutes), the crystal drive was tuned and the period recorded. The period of the specimen was then compared to the period of the crystals alone; in order to determine the validity of such tests, a ratio of only 0.95-1.05 between the two periods is desired. Furthermore, the spacer rod (c.s.r) serves the purpose of keeping the quartz crystals at room temperature, while the specimen is at high or elevated temperature. The ceramic spacer rod must be tuned to resonate for the frequency of the quarts crystals being used and for the particular temperature of the tests and the adhered joint between the specimen and the c.s.r. is made with sauereisen cement.

The electrical system is driven by a closed loop oscillator at a pre-selected gauge crystal voltage (V_g) and constant maximum strain amplitude (ε_{amp}) in the specimen.

The available frequencies with the technique is in the range of 20 to 200 KHz. In typical tests, the values of the drive and gauge crystal voltage V_d, and V_g, respectively, and the resonant period R_{pd} of the four component system were measured. These data with the individual masses m (i), where i = d, g, c.s.r, or p, and the values of the resonant period of the driver and gauge crystal, or driver, gauge, spacer rod, were also measured before the specimen was attached, using the closed loop crystal driven and a frequency counter, and the length of the specimen (*L*), permitted the calculation of the dynamic Young's modulus (E_d) of the tested composite specimen using the standard equations 2 and 3, ref[11,12,16,18].

$$R_{pd}(p) = \frac{(\sqrt{m_p})R_{pd}(d_g R_{c.s.r})R_{pd}(d_g R_{c.s.r}\, p)}{C} \qquad (2)$$

Where *C* is given by:

$$C = \sqrt{R_{pd}^2(d_g R_{c.s.r})m(d_g R_{c.s.r} P) - R_{pd}^2(d_g R_{c.s.r} P)m(d_g R_{c.s.r})}$$

$$E_d = {4\rho L^2}\big/{R_{pd}^2(P)} \qquad (3)$$

Corrections were made for changes in density (ρ) and length of the composite specimen at elevated temperature by including the coefficient of thermal expansion in the equations, in this study, the range of strain amplitudes (ε_a) investigated using this technique falls between 10^{-7} and 10^{-2}. The vibrational frequency controlled by the length of the quartz crystal was 80 KHz.

3. Results and Discussion

The average values of modulus for the tested composite materials at room and elevated temperatures are shown in Table 3 for both longitudinal (II) and transverse ($\perp$) fiber orientation. Figures (2, 3, 4, 5 and 6) show the temperature dependence of modulus for the tested MMC materials. Linear regression was used to determine the equation of a line which would most closely approximate the temperature dependence of the modulus for each material.

Table 3: The average values of modulus at room and elevated temperature for the tested composite materials.

Type of composite material	Fibre orientation	Modulus at T_{room} (GPa)	Modulus at $T_{450°C}$ (GPa)
55 v/o Al_{pure}-Al_2O_3	II	235.3	148.7
	$\perp$	140	56.4
55 v/o Al_{alloy}-Al_2O_3	II	210.5	122
	$\perp$	123	39.4
55 v/o Al_{pure}-B	II	216	92
	$\perp$	134	55
55 v/o Al_{alloy}-B	II	186.6	78
	$\perp$	115	47.4
55 v/o Al_{pure}-W	II	169	68.9
	$\perp$	123	50
55 v/o Al_{alloy}-W	II	151	62
	$\perp$	111	45
55 v/o Al_{pure}-SiC	II	132	99.5
	$\perp$	96.5	73.7
55 v/o Al_{alloy}-SiC	II	119	79
	$\perp$	108	89.5
55 v/o Al_{pure}-H.S.C	II	178	147
	$\perp$	102	98.8
55 v/o Al_{alloy}-H.S.C	II	152	136
	$\perp$	115	119

  - Volume 2, Number 1 (ISSN 1995-6665)

The resulting equations are listed in Table 4 along with the coefficient of determination (R^2). The temperature dependence of the modulus ranged from -0.0428 to -13.66 GPa /ºC (which represent the lowest and highest slope values obtained from E vs. T graphs, Fig's.2-5) for Al_{pure} and Al_{alloy} metal matrix reinforced Al_2O_3, B, W and SiC fibre composite materials, Table 4. In contrast, however, the H.S.C-Al composite materials showed a nonlinear temperature dependence of modulus behavior and polynomial regression was used. The boron fiber reinforced Al and Al_{alloy} specimens showed the greatest loss of modulus with respect to temperature.

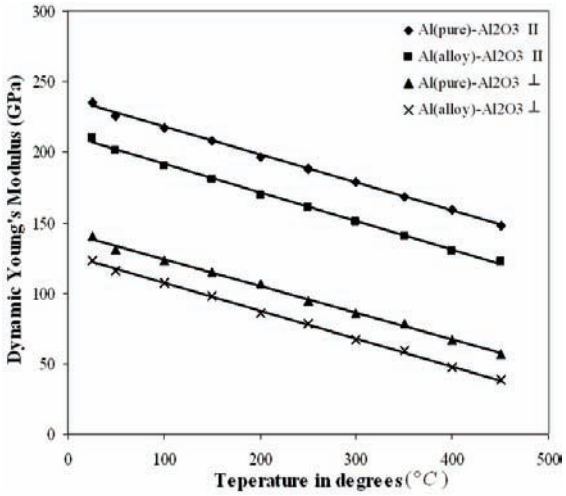

Figure 2: Temperature dependence of longitudinal (II) and transverse ($\perp$) dynamic modulus for Al_2O_3-Al_{pure} and Al_{alloy} matrix composites.

Table 4 also includes the values of the parameter $-(10^4/E(T_{test}))(dE/dT)$, at 25 ºC, which represents the normalized fall-off in modulus at temperature increases. The values for SiC (II and $\perp$), and Al_2O_3 (II) fiber reinforced Al and Al_{alloy} are in the range of 5×10^{-5} to $10\times10^{-4}\,^{\circ}C^{-1}$ and this agrees with the range of values noted by, [13], for many metals at room temperature. For these two particular fiber oriented composite material, it seems that the decrease in modulus with increasing test temperature can be attributed mostly to the matrix material.

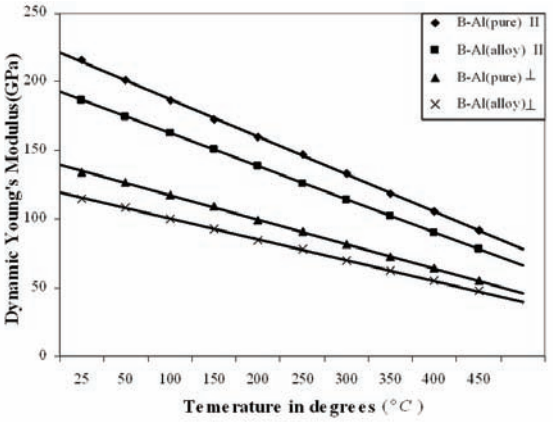

Figure 3: Temperature dependence of longitudinal (II) and transverse ($\perp$) dynamic modulus for B-Al_{pure} and Al_{alloy} matrix composites.

It has been suggested by, [3, 5, 13, and 26], that the presence of a strong fiber-matrix interfacial strength which exists in SiC and Al_2O_3 fiber reinforced Al_{alloy} matrix composite materials, (which occurs due to fiber-matrix interfacial reaction), has a detrimental effect on composite mechanical properties. The correlation among the melting point (T_m), the modulus and interatomic forces in materials is another contributing factor for this type of behavior, making the fall-off in modulus for Al high, ($(T_{test}/T_{melting})$ approaches 0.7), and the fall-off for SiC low, ($(T_{test}/T_{melting})$ approximately 0.22).

Table 4. Modulus-Temperature Equations and parameter [–(1/E (0)) (dE/dT)].

Figure number	Type of composite material	Fiber orientation	Equation, E in (GPa) ; T in (°C) **[E(T) = ….]**	(R^2)	$-\left(\frac{10^4}{E(T)}\right)\left(\frac{dE}{dT}\right)$ (K^{-1})
Fig. no. 2	55 v/o Al_{pure}-Al_2O_3	II	237.59 -0.198 T	0.998	8.52
		$\perp$	142.8 -0.19 T	0.997	13.76
	55 v/o Al_{alloy}-Al_2O_3	II	211.81 -0.204 T	0.997	9.87
		$\perp$	126.7 -0.1967 T	0.999	16.14
Fig. no. 3	55 v/o Al_{pure}-B	II	288.5 -13.66 T	0.999	53.7
		$\perp$	144.43 -8.89 T	0.999	72.81
	55 v/o Al_{alloy}-B	II	199.4 -12.13 T	0.999	70.82
		$\perp$	122.8 -7.541 T	0.999	72.14
Fig. no. 5	55 v/o Al_{pure}-W	II	170.99 -0.229 T	0.988	13.86
		$\perp$	124.6 -0.167 T	0.990	13.86
	55 v/o Al_{alloy}-W	II	152.43 -0.205 T	0.997	13.92
		$\perp$	108.2 -0.1604 T	0.816	15.39
Fig. no. 4	55 v/o Al_{pure}-SiC	II	134.62 -0.077 T	0.975	5.88
		$\perp$	97.13 -0.0509 T	0.998	5.31
	55 v/o Al_{alloy}-SiC	II	120.1 -0.0924 T	0.995	7.84
		$\perp$	108.61 -0.0428 T	0.992	3.98
Fig. no. 6	55 v/o Al_{pure}-H.S.C	II	208.2 -$(3\times10^{-7})T^4$ -$(7\times10^{-6})T^3$ +0.013 T^2 -1.57 T	0.933	52.48
		$\perp$	85.98 -$(8\times10^{-7})T^4$ +0.0002 T^3 +0.022 T^2 -1.096 T	0.823	30.57
	55 v/o Al_{alloy}-H.S.C	II	186.6 +$(1\times10^{-6})T^4$ -0.0003 T^3 +0.044 T^2 -2.28 T	0.928	39.68
		$\perp$	126 -$(6\times10^{-8})T^4$ -$(1\times10^{-5})T^3$ +0.006 T^2 -0.546 T	0.879	23.14

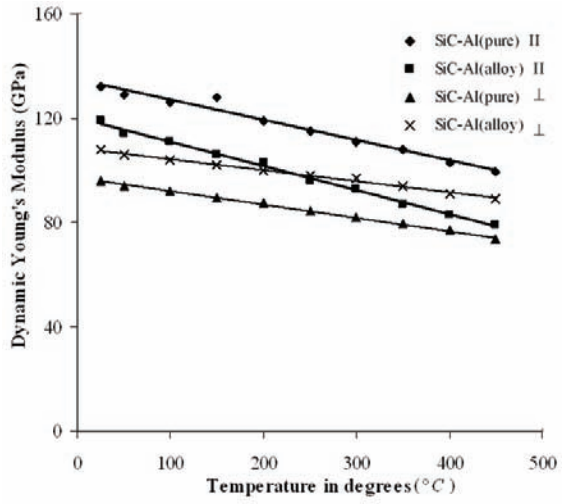

Figure 4: Temperature dependence of longitudinal (II) and transverse ($\perp$) dynamic modulus for SiC-Al_{pure} and Al_{alloy} matrix composites.

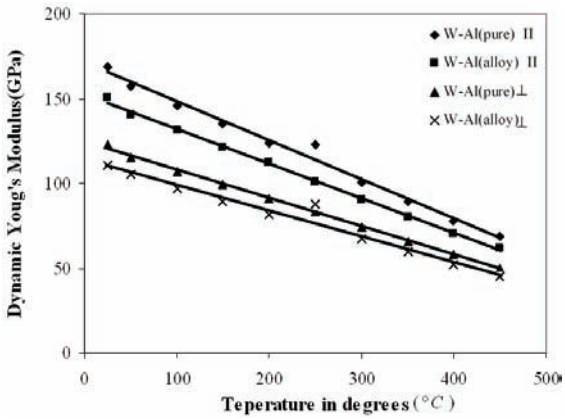

Figure 5: Temperature dependence of longitudinal (II) and transverse ($\perp$) dynamic modulus for W-Al_{pure} and Al_{alloy} matrix composites.

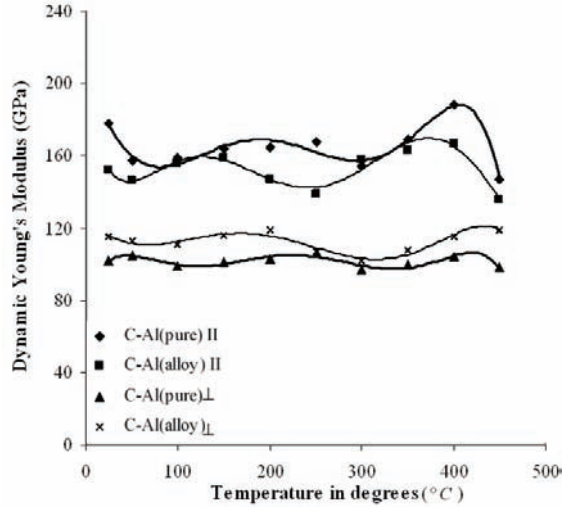

Figure 6: Temperature dependence of longitudinal (II) and transverse ($\perp$) dynamic modulus for H.S.C-Al_{pure} and Al_{alloy} matrix composites.

Figure 6 presents the modulus as a function of temperature for H.S.C fiber reinforced Al and Al_{alloy} matrix composites, where the presence of H.S.C reinforcement has led to a non-monotonic decrease in modulus in both II and $\perp$ fiber directions. A specimen from H.S.C-Al_{pure} and H.S.C-Al_{alloy} composite plates were tested with each specimen being tested over the temperature range of 25 to 450 ºC, and then retested over the range of 50 to 400 ºC. A second specimen was tested over a 25 to 450 ºC temperature range. For all tests, the modulus first decreased to a minimum of 154 GPa as the temperature increased, and then increased to a maximum of 188 GPa at 400 ºC for H.S.C-Al_{pure}, and for H.S.C-Al_{alloy} composite plate from a minimum of 136 GPa (at 250 ºC) to 167 GPa (at 400 ºC). From the obtained results, it is evident that there was a non-monotonic response of modulus with temperature, and a hysteresis effect with respect to thermal cycling has resulted in different responses as successive runs were carried on the same specimen.

The non-monotonic behavior has also been observed for Gr-Al composite system by, [14, 20], in which the modulus decreased with decreasing temperature over the range of 80 to -60 ºC. This behavior may be attributed to the strong dependence of the modulus of the fiber on residual stresses that exist at fiber-matrix interface as a result of the mismatch of coefficients of thermal expansivity (CTE) between fiber and matrix (carbon has negative CTE, -0.4 to -1.2). However, it is possible that successive thermal cycling may have alleviated the residual stresses, possibly through dislocation generation, [8], and reduced the amount of initial modulus loss.

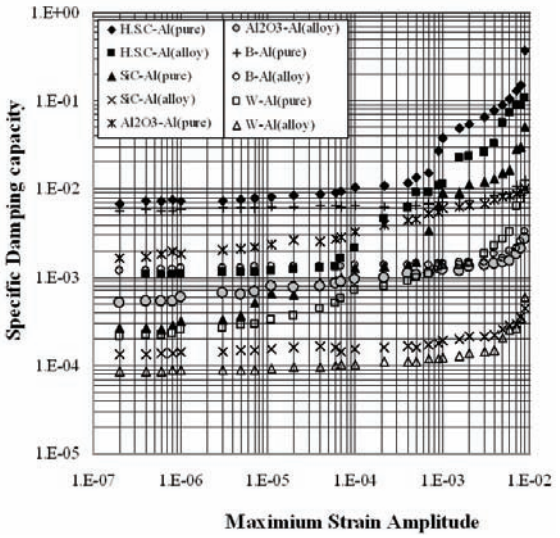

Figure 7: Strain dependence of mechanical damping at room temperature in the tested Al_{pure} and Al_{alloy} matrix composites with fiber volume fraction of 50%. (80 to 150 kHz longitudinal vibration mode).

The strain amplitude dependence of damping was investigated for all MMC tested specimens with results shown in Figures 7 and 8. The B- Al_{pure}, B- Al_{alloy}, SiC-Al_{alloy}, and Al2O3- Al_{alloy} composite specimens, as in Fig.7, exhibited a strain amplitude independent behavior over a strain range of 10^{-7} to 10^{-4} and a slight nonlinear amplitude dependent damping at higher strain amplitude of

10^{-2}. The damping data for fiber reinforced Al_{pure} matrix composite materials; show a small region of strain amplitude independent damping at low strains 10^{-7} - 10^{-6} , followed by a region of nonlinear, amplitude dependent damping at higher strains of 10^{-6} - 10^{-2} strain amplitude. In the composite systems with no strain amplitude dependence were observed, it is unlikely that interfacial friction (i.e. frictional sliding) is responsible in these types of composites, however, it is possible that interfacial microplasticity or matrix microcracking is responsible.

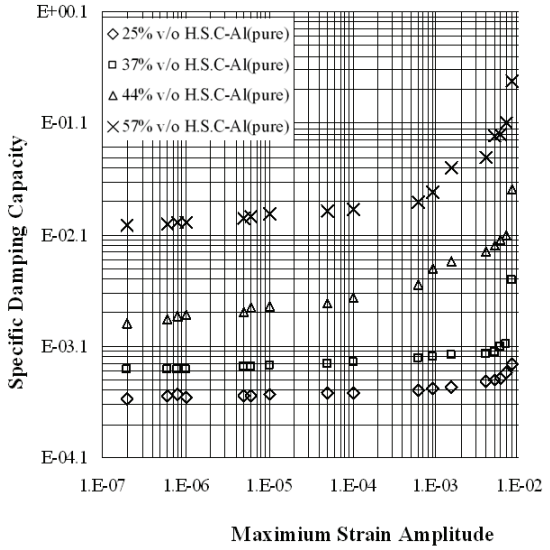

Figure 8: Strain dependence of mechanical damping at T_{room} in H.S.C-Al_{pure} matrix composites. (80 to 150 KHz longitudinal vibration mode).

It is apparent that in the case of ceramic fiber reinforced Al_{pure}, and in some cases Al_{alloy} metal matrix composites, the relatively large difference between CTE's for the fiber and matrix caused a rise in thermal stresses during the cooling process of the fabricated specimens, resulting in a high dislocation density near fiber-matrix region (i.e. frictional bonding has occurred). It can be suggested that fiber-matrix frictional sliding, (due to the presence of weak fiber-matrix interfacial bonding), has led to enhance damping at high frequency and low strain amplitudes 10^{-7} - 10^{-2}. These observations are in agreement with previous studies on SiC and C fiber reinforced Al metal matrix composite systems by [5] which indicated that the high impact and tensile strength in the longitudinal fiber direction reinforcement is mainly due to the presence of energy absorbing mechanisms, such as matrix ductility and fiber-matrix weak interfacial strength are responsible for the improved mechanical properties. Further investigation on the effect of matrix ductility and fiber-matrix interfacial region on damping were carried out, the trend here is to increase fiber volume fraction of H.S.C-Al_{pure} metal matrix composite ranging from 25% to 57% v/o, in order to increase the fiber-matrix interface area. It was clear from Fig. 8, that this (increasing the percentage of fiber v/o) has resulted in strain amplitude dependence, which clearly means that increasing fiber-matrix interfacial area in frictionally bonded composite materials, and increasing matrix ductility will enhance damping levels in such tailor made composites.

The obtained results for W-Al composite material, Figures (5 and 7), show that in spite of the large difference between matrix and fiber CTE's, a less severe modulus between fiber and matrix than in the ceramic fiber case may have led to the reduced interfacial sliding. Henceforth, it can be said that increasing fiber-matrix interface and matrix ductility in the studied MMC's did translate into increased damping. However, more detailed studies of interactions at the interface region are needed in order to further understand the damping behavior and effectively design composites with increased damping.

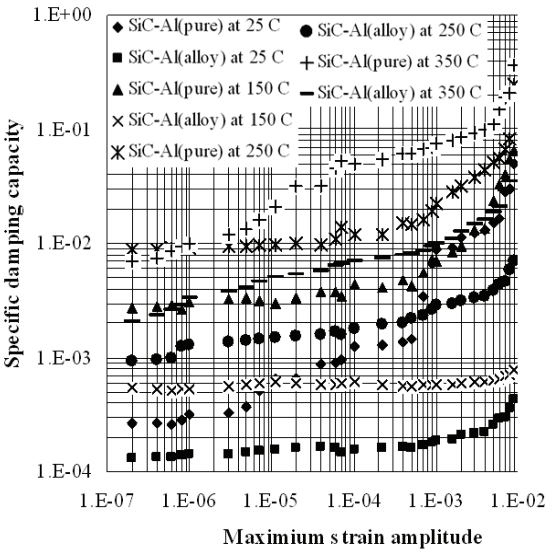

Figure 9: Strain dependence of mechanical damping at room and elevated temperature in SiC-Al_{pure} and Al_{alloy} matrix composites with fiber volume fraction of 30%. (80 to 150 KHz, longitudinal vibration mode).

The strain amplitude dependence of mechanical damping in the longitudinal vibration mode in the temperature range of 25 to 350 ºC, for H.S.C-Al_{pure} matrix composite, is shown in Fig.9. It is evident that increasing composite matrix ductility seems to further weaken the fiber-matrix interfacial region, resulting in higher specific damping values particularly at increasing strain amplitude. From these results it is also apparent that continuous ceramic fiber reinforced MMC's retain their mechanical properties and thermal stability even at elevated temperatures because any interaction between fiber and matrix constituents occurs very slowly in the solid state.

Little or no information were reported in the literature pertinent to temperature dependence of dynamic modulus and damping for continuous fiber reinforced metal matrix materials at elevated temperature. Previous studies, [20-25], on temperature dependence of dynamic modulus and damping were all carried out at room temperature and on either whisker or discontinuous fiber reinforced metal matrix composites. Therefore, making these results obtained in this paper, to be the first such reported information for continuous ceramic fiber reinforced MMC's at elevated temperatures.

4. Conclusions

The dynamic modulus in the longitudinal (II) and transverse ($\perp$) fiber direction, and mechanical damping in the longitudinal vibration mode only, were measured for the tested MMC's at room and elevated temperatures and conducted at up to 150 kHz. The temperature dependence of dynamic modulus in all tested MMC's showed a linear, monotonic decrease in modulus with increase in temperature, except in the case of H.S.C-Al_{pure} and Al_{alloy} matrix composites, the presence of H.S.C fibre reinforcement has led to a non-monotonic decrease in modulus.

The obtained results for fiber reinforced Al_{pure} matrix composites, showed a strain amplitude dependent damping at room temperature, while the B, SiC, and Al_2O_3, fiber reinforced Al_{alloy} matrix material exhibited essentially an amplitude independent damping at high strain amplitudes. At lower strain amplitudes, these composites became strain amplitude dependent on damping.

Increasing the volume fraction of high strength carbon fiber in Al_{pure} matrix in the range of 25 to 57%, has resulted in increasing the fiber-matrix interfacial areas, this seems to be effective in increasing the damping in such composites. The measured longitudinal vibration mode of damping for H.S.C-Al_{pure} matrix composite at temperature in the range of 25 to 350 ºC has shown to exhibit strain amplitude dependent damping.

References

[1] Ming Yang, V.D. Scott and R.L.Trumper, "The role of interface on the mechanical behaviour of carbon fibre reinforced aluminium alloy composites". Metal Matrix Composites 2nd Conference. The Royal Society, U.K, 1989.

[2] Evans A, March, C.S, Mortensen. Metal Matrix Composites in industry. An Introduction and Survey. Klumer Academic Publisher; 2003, 375-386.

[3] Arsenault, R.J. and Fisher, R.M. , " Microstructure of fibre and particulate SiC in 6061 Al composites. Scripta. Met. Vol.17, 1983,67-71.

[4] Hunt, W.H. Interfacial zones and mechanical properties in continuous fiber FP/Al-Li metal matrix composites. In: Dhingra and Fishman. Interfaces in metal matrix composites. (, Warrendale: Met. Soc.AIME; 1986, 3-25.

[5] Ramadan J. Mustafa and Yassin L. Nimir, "A New Process for Manufacturing Continuously Reinforced Aluminium Alloy MMC". Mu'tah Lil-Buhuth wad-Dirasat (Mu'tah Journal for Research and Studies), Natural and Applied Sciences Series, Vol.21, No. 2, 2006, 183-206.

[6] P.J. de Groot, P.M. Wijnen, and R.B.F. Janssen,"Real-Time Frequency Determination of Acoustic Emission for Different Fracture Mechanics Carbon/Epoxy Composites".Comp. Sci. and Tech.,Vol.55 , 1995, 405-412

[7] M. V. Lysak, Development of the theory of Acoustic Emission by Propagating Cracks in Terms of Fracture Mechanics. Eng. Fracture Mechanics, Vol.55, No.6,. 1996, 443-452.

[8] M. Radovic, E. Lara-Curzio, L.Riester in "Comparison of Different Experimental Techniques for Determination of Elastic Properties of Solids". Material Science and Eng., 368, 2004, 56-70.

[9] Granato, A. and Lucke, K.," Application of dislocation theory to internal friction phenomena at high frequencies". Journal of Applied Phyiscs, Vol.27, 1956b,789-805.

[10] Markham, M. F. Measurement of the elastic constants of fibre composites by ultrasonic. Composites, Part A; 1970.

[11] Robinson, W.H. and Edgar A.," The piezoelectric method of determining mechanical damping at frequencies of 30 to 200KHz". IEEE Trans. Sonics and Ultrasonic SU-Vol. 21,1974, 98-105.

[12] Lin, D. X., R. G. Ni and R. C. Adams.," Prediction and Measurement of the Vibrational Damping Parameters of Carbon and Glass Fibre Reinforced Plastic Plates". J. Composite Materials, Vol.18, No.2, 1984,132-152.

[13] Friedel, J. Dislocations. Vol.3, New York.: Pergammon Press, ;1964; pp. 454-457.

[14] Audoin B., Baste S., "Ultrasonic evaluation of stiffness tensor changes and associated anisotropic damage in a ceramic matrix composite". Journal of Applied Mechanics, Vol. 59, 1994, 445-448

[15] Ni, R. G. and R. C. Adams, " The Damping and Dynamic Moduli of Symmetric Laminated Composite Beams-Theoretical and Experimental Results". Journal Composite Materials, Vol.18, No.2, 1984, 104-121.

[16] Schoenberg, T. Boron and Silicon Carbide fibres.In: C.A Dostal. Composites, Vol. 1 , Ohio: ASM International, Metals Parks; 1987, 54-65.

[17] ASM Engineered Materials Handbook, Composites ,Vol.1, ASM International Metals, Metals Park, Ohio,1987.

[18] J.R. Davis (Ed), Metals Handbook, ASM International, Materials Park; Ohio, 1990.

[19] Harmouche, M., and Wolfenden, A., "Temperature and Composition Dependence of Young's Modulus for Ordered B2 polycrystalline CoAl and FeAl". Mat. Sci, Eng A, Vol.84, 1986, 35-41.

[20] Liu, J.M. "Temperature dependence and hysteresis of Young's modulus in a graphite/aluminum metal matrix composite". Appl. Phys. Lett. Vol.48, 1986, 469-471

[21] Castagnede B., Jenkings, J. T., Sachse W., Baste S. "Optimal determination of the elastic constants of composite materials from ultrasonic wave-speed measurements". Journal of Applied Physics, Vol. 67, 1990, 657-665

[22] H.W. Viehrig, K.Popp, and R. Rintamaa, Measurement of Dynamic Elastic-Plastic Fracture Toughness Parameters Using Various Methods, Int. J. Press. Ves. And Piping, Vol. 55 ,1993, 233-241.

[23] Sahay, S, Kline R., Mignogna, R.," Phase and group velocity considerations for dynamic modulus measurements in anisotropic media". Ultrasonic, Vol. 30., No. 6, 1992, 373-382.

[24] Hufenbach, W., Langkamp, A., Kroll, L., Bohm, R., "Experimental investigation and modeling of failure and damage behaviour of multi-layered carbon fibre reinforced". PEEK14thInternational Conference on Composite Materials Proceedings (ICCM 14), San Diego, USA, 2003.

[25] Hufenbach, W., Bohm, R., Kroll, L., Langkamp, A., "Theoretical and experimental investigation of anisotropic damage in textile reinforced composite structures". Mechanics of Composites, Vol. 40, No.6, 2004,.519-532.

[26] Ramadan. J. Mustafa and Yassin L. Nimir, "The Fracture Behaviour of Continuous SiC and Carbon Fibre Al-Matrix Composites under Mode II Loading Conditions". Mu'tah Lil-Buhuth wad-Dirasat (Mu'tah Journal for Research and Studies), Natural and Applied Sciences Series, Vol.18, No.1, 2003.

.